Published OnlineFirst November 1, 2019; DOI: 10.1158/0008-5472.CAN-18-3241

Twist1-Induced Epithelial Dissemination Requires Prkd1 Signaling

Dan Georgess[1,2], Veena Padmanaban[1], Orit Katarina Sirka[1], Kester Coutinho[1], Alex Choi[1], Gabriela Frid[1], Neil M. Neumann[1], Takanari Inoue[1], and Andrew J. Ewald[1,3,4]

ABSTRACT

Dissemination is an essential early step in metastasis but its molecular basis remains incompletely understood. To define the essential targetable effectors of this process, we developed a 3D mammary epithelial culture model, in which dissemination is induced by overexpression of the transcription factor Twist1. Transcriptomic analysis and ChIP-PCR together demonstrated that protein kinase D1 (Prkd1) is a direct transcriptional target of Twist1 and is not expressed in the normal mammary epithelium. Pharmacologic and genetic inhibition of Prkd1 in the Twist1-induced dissemination model demonstrated that Prkd1 was required for cells to initiate extracellular matrix (ECM)–directed protrusions, release from the epithelium, and migrate through the ECM. Antibody-based protein profiling revealed that Prkd1 induced broad phosphorylation changes, including an inactivating phosphorylation of β-catenin and two microtubule depolymerizing phosphorylations of Tau, potentially explaining the release of cell–cell contacts and persistent activation of Prkd1. In patients with breast cancer, *TWIST1* and *PRKD1* expression correlated with metastatic recurrence, particularly in basal breast cancer. Prkd1 knockdown was sufficient to block dissemination of both murine and human mammary tumor organoids. Finally, *Prkd1* knockdown *in vivo* blocked primary tumor invasion and distant metastasis in a mouse model of basal breast cancer. Collectively, these data identify Prkd1 as a novel and targetable signaling node downstream of Twist1 that is required for epithelial invasion and dissemination.

Significance: Twist1 is a known regulator of metastatic cell behaviors but not directly targetable. This study provides a molecular explanation for how Twist1-induced dissemination works and demonstrates that it can be targeted.

Graphical Abstract: http://cancerres.aacrjournals.org/content/canres/80/2/204/F1.large.jpg.

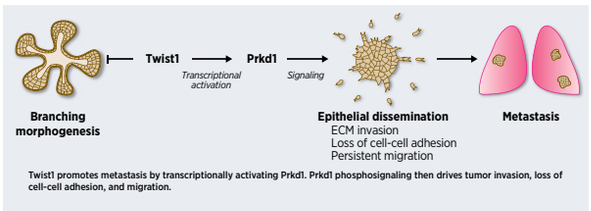

Introduction

Metastasis is the major driver of mortality across cancer sites (1). Metastasis requires cancer cells to escape the primary tumor and disseminate into the stroma (2), enter the systemic circulation, and colonize distant organs (3). Dissemination can be triggered by expression of transcription factors, such as Twist1, via an epithelial-to-mesenchymal transition (4). However, Twist1 can also induce the dissemination of epithelial phenotype cells that retain cytokeratins and E-cadherin (5, 6). The concept of dissemination of epithelial phenotype cancer cells has clinical support, as most breast tumors are invasive ductal carcinomas and retain E-cadherin expression in primary tumors and metastases (7, 8). Circulating tumor cells can also express Twist1 and epithelial markers (9), with or without broader induction of mesenchymal markers (10). Clinical and experimental studies therefore support a mechanism for dissemination and metastasis by cells without a complete EMT. We set out to define the targetable molecular effectors of this mechanism.

We use Tet-inducible Twist1 expressing mammary organoids as a model system for dissemination, as Twist1 is not expressed in adult epithelia (11) but is highly expressed in diverse invasive cancers (4, 12, 13) and correlates with poor patient outcomes (14–16). We build on those differential expression results to identify novel transcriptional and signaling mechanisms that are required for epithelial dissemination. We first used pharmacologic inhibitors to test the requirement for various Twist1-upregulated genes, eventually focusing on protein kinase D1 (Prkd1). Prkd1 (originally PKCμ; ref. 17) is a serine/threonine kinase and the founding member of the Prkd family, which includes Prkd2 and Prkd3 (18). At the signaling level, activators of Prkd1 include Prkc and microtubule depolymerization (19, 20). Accordingly, we assessed the involvement of Prkc and microtubule dynamics in the dissemination of Twist1$^+$/Prkd1$^+$ epithelial cells. We also used antibody-based protein profiling to characterize Prkd1-dependent downstream signaling with

[1]Department of Cell Biology, Center for Cell Dynamics, Johns Hopkins University School of Medicine, Baltimore, Maryland. [2]Department of Natural Sciences, School of Arts and Sciences, Lebanese American University, Beirut, Lebanon. [3]Department of Biomedical Engineering, Johns Hopkins University School of Medicine, Baltimore, Maryland. [4]Cancer Invasion and Metastasis Program, Department of Oncology, Sidney Kimmel Comprehensive Cancer Center, Johns Hopkins University School of Medicine, Baltimore, MD 21205.

Note: Supplementary data for this article are available at Cancer Research Online (http://cancerres.aacrjournals.org/).

Material requests should be addressed to A.J. Ewald.

Corresponding Authors: Andrew J. Ewald, Center for Cell Dynamics, Johns Hopkins University School of Medicine, 855 N. Wolfe Street, 452 Rangos Bldg., Baltimore, MD 21205. Phone: 410-614-9288; E-mail: andrew.ewald@jhmi.edu; and Dan Georgess, Department of Natural Sciences, Lebanese American University, Madame Curie Street, P.O. Box 13-5053/F63, Beirut, Lebanon. Phone: 961-178-6456, ext. 3951; E-mail: dan.georgess@lau.edu.lb

Cancer Res 2020;80:204–18

doi: 10.1158/0008-5472.CAN-18-3241

Published OnlineFirst November 1, 2019; DOI: 10.1158/0008-5472.CAN-18-3241

the goal of explaining the regulation of distinct dissemination steps. Finally, we demonstrated Prkd1's requirement for dissemination of murine and human mammary tumor organoids in culture, and for both primary tumor invasion and distant metastasis in a basal breast cancer model *in vivo*.

Materials and Methods

Mice

All mice used in this study were backcrossed onto and maintained on the FVB/n background, in a specific pathogen-free facility. Animal procedures were conducted in accordance with protocols approved by the Johns Hopkins Animal Care and Use Committee. The CMV::rtTA; TetO-Twist1 (Twist1-inducible) mouse strain was obtained as described previously (5, 6). The MMTV-PyMT [FVB/N-Tg (MMTV-PyVT)634Mul/J; ref. 21], C3(1)-TAg [FVB-Tg(C3-1-TAg) cJeg/JegJ; ref. 22], and mTmG (23) mouse lines were obtained from The Jackson Laboratory. The C3(1)TAg;mTmG was obtained by crossing the C3(1)-TAg and mTmG lines.

Isolation and 3D culture of murine mammary tissues

Murine Twist1-inducible (CMV::rtTA;TetO-Twist1) and tumor [MMTV-PyMT and C3(1)-TAg] organoids were isolated and cultured following the protocol for wild-type mouse mammary gland culture (detailed protocol in ref. 24). Briefly, mammary glands or tumors were harvested from 8- to 24-week-old mice, fragmented into epithelial organoids by mechanical disruption and collagenase/trypsin digestion, then separated from single cells by three differential centrifugations (3 seconds, 430 × *g*). Twist1-inducible organoids were embedded in growth factor reduced Matrigel (Corning 354230). Tumor organoids were embedded in fibrillar type I rat tail collagen gels (Corning 354236; ref. 24). Organoid–matrix suspensions (1–2 organoids/μL) were seeded in 24-well coverslip bottom plates (Greiner Bio One 662892) and supplemented with media as detailed in ref. 24. For activation of Twist1 expression in CMV::rtTA;TetO-Twist1 organoids, culture medium was supplemented with 5 μg/mL doxycycline (Shanghai RenYoung Pharmaceutical Co., Ltd) and replaced every 48 hours. For Supplementary Fig. S1, soluble recombinant TGFβ1 (PeproTech 100-21) was used at 2.5 ng/mL.

Isolation and 3D culture of fresh primary human tumors

Primary breast tumors were acquired from the Cooperative Human Tissue Network in accordance with a study protocol (NA_00077976) that was acknowledged as exempt/not human subjects research by the Johns Hopkins School of Medicine Institutional Review Board. In brief, each tumor sample was deidentified by the CHTN prior to shipment with limited prespecified clinical information provided with the sample. Tumor samples were shipped in DMEM or RPMI. Upon receipt, each tumor sample was washed in antibiotic and fungizone, then minced, and digested in collagenase (Sigma-Aldrich C2139; ref. 25). Tumor organoids were then purified and embedded in collagen following the protocols for murine tumor organoids (see previous paragraph). After collagen polymerization, medium containing insulin, EGF, hydrocortisone, and cholera toxin was added (25). Human tumor organoid cultures were maintained for 3 to 4 days.

RNA sequencing dataset

The dataset was obtained from ref. 5 and is publicly available (Sequence Read Archive accession no. SRP033275). In the current study, we utilized the list of 106 Twist1-upregulated transcripts (excluding Twist1 itself) that were differentially expressed at genome-wide significance (5).

Twist1-induced dissemination assay

Twist1-inducible organoids were cultured for 7 days in organoid culture medium supplemented with doxycycline to induce Twist1 expression (5, 6). For the small-molecule inhibition assay in **Fig. 1A** and Supplementary Fig. S2, organoids were treated with individual drugs at 5 doses (0, 10 nmol/L, 100 nmol/L, 1 μmol/L, 10 μmol/L), starting from day 0 (Supplementary Table S1). Equal concentrations of the universal vehicle, DMSO, were maintained across all drug dose conditions. Media (including drug and doxycycline) were replenished every 48 hours, as doxycycline is labile. Endpoint (day 7) images were collected for 20 to 40 organoids per condition across biological replicates. For each drug, at least 3 biological replicates were used, consisting of organoid cultures from independent mice. The number of disseminated cells per organoid was counted manually using Fiji. Normalized dissemination (%) for each organoid within a biological replicate was obtained by dividing the number of disseminated cells by the median in the 0 nmol/L (vehicle control) condition. Normalized dissemination values were pooled across biological replicates and curve-fitted using the "log(inhibitor) versus normalized response – variable slope" function in Prism 7 (GraphPad) according to the following formula: $Y = 100/(1+10\text{^}((\text{LogIC}_{50}\text{-X})^{*}\text{HillSlope}))$, where Y = log(drug concentration) and X = normalized dissemination. No constraints were applied to the Hill slope or any other variable in the curve fit. This allowed the calculation of the IC_{50} for each drug. When a drug treatment did not reduce dissemination, curve fits were impossible to generate and drugs were indicated in **Fig. 1B** (top right corner; "No inhibition" box). Multi-drug comparison (**Fig. 1B**) was performed by plotting IC_{50} and dissemination at 1 μmol/L for individual drugs. Drugs were considered as potent inhibitors of dissemination if $IC_{50} < 1$ μmol/L and dissemination at 1 μmol/L was <33% (**Fig. 1B′**).

Organoid growth assay

In **Fig. 2E–F'** and Supplementary Fig. S1E, Twist1-inducible organoids were cultured for 7 days without addition of doxycycline, that is, in the Twist1-Off condition, equivalent to wild-type mammary organoids. Paired images for each organoid were acquired on day 0, day 3 (optional), and day 7 of culture. For each organoid, the contour at each time point was determined manually in Fiji, and a growth fold change was calculated as the ratio of projected surface areas from a given time point over that of day 0.

Early invasion and dissemination in Twist1-inducible organoids

In **Fig. 3A** and **B**, Twist1-inducible organoids were imaged using time-lapse DIC microscopy at 20-minute intervals for the first 60 hours immediately following doxycycline (for Twist1 induction) and vehicle (DMSO) or Gö-6976 (330 nmol/L or 3.3 μmol/L). Image analysis was performed with Fiji. Organoids with cells extending visible ECM-directed protrusions at the final time point were considered invasive and scored as a percentage of total organoids imaged. Cells that detached from organoids across the entire 60 h interval were considered disseminating.

Cell migration in Twist1-inducible organoids

In **Fig. 3E** and **F**, Twist1-inducible organoids were imaged using time-lapse DIC microscopy for a total of 140 hours at 20-minute time intervals. For the first 70 hours, all organoids were treated with

Published OnlineFirst November 1, 2019; DOI: 10.1158/0008-5472.CAN-18-3241

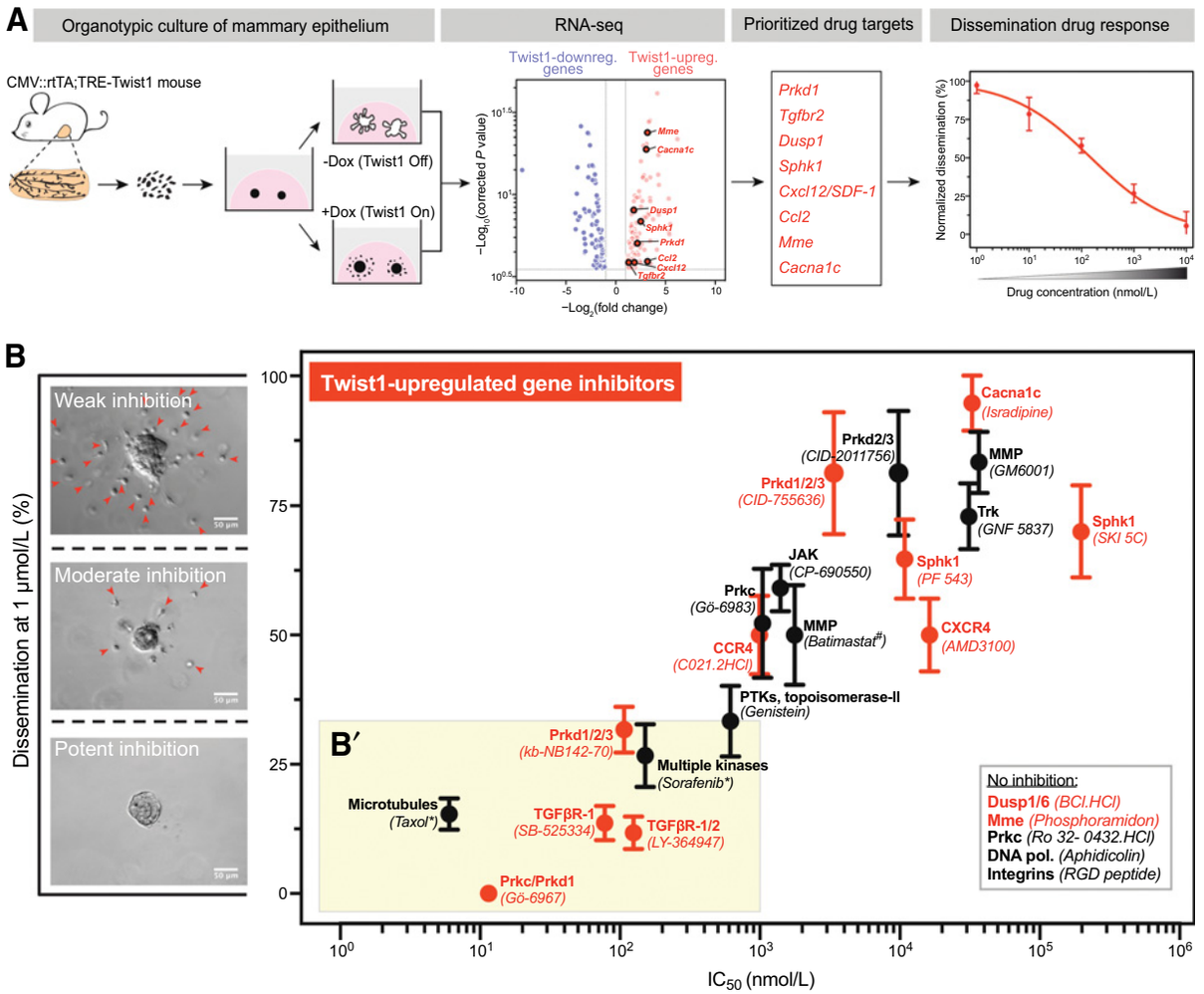

Figure 1.

Identification of targetable molecular requirements for Twist1-induced epithelial dissemination. **A,** Schematic representation of our experimental pipeline. Mammary organoids from Twist1-inducible transgenic mice were cultured without (Twist1-Off) or with (Twist1-On) doxycycline to induce Tet-activated Twist1 expression. Differential RNA-seq of these organoids identified Twist1-upregulated (red) and downregulated (blue) genes, represented here as a volcano plot, where the reported *P* value was corrected for multiple testing (dataset, *P* values and fold changes obtained from ref. 5). The Twist1-upregulated gene set was prioritized for functional investigation (full list of small molecules and corresponding targets can be found in Supplementary Table S1). Each small molecule was tested at 5 concentrations (0, 10, 100, 1,000, and 10,000 nmol/L) in Twist1-On organoids. For each dose, the number of disseminated cells per organoid was normalized to that of the vehicle control (0 nmol/L), then curve-fitted with a Hill dose–response function. **B,** Plot representing IC_{50} and dissemination at 1 µmol/L for individual small molecules (and corresponding target proteins) used in the Twist1-induced dissemination assay (**A**). For each compound, $n \geq 20$ organoids per mouse per dose, $r = 3$ mice, Tested molecules include Twist1-predicted inhibitors (red) and non-Twist1–predicted inhibitors (black; detailed in Supplementary Table S1). *, FDA-approved drugs. #, data values from ref. 6. Error bars, SEM. To the left of the *y*-axis, representative DIC micrographs display the range of dissemination inhibition. Red arrowheads, disseminated cells. Scale bars, 50 µm. **B′,** Potent inhibitors with IC_{50} < 1,000 nmol/L and dissemination at 1 µmol/L < 33.3% (yellow box).

doxycycline to induce Twist1 expression. Doxycycline-containing organoid media was replenished and supplemented with either vehicle (DMSO) or Gö-6976 (330 nmol/L or 3.3 µmol/L) either at 0 hours (**Fig. 3A** and **B**) or at 70 hours (**Fig. 3E** and **F**) of culture. Single-cell tracking and speed velocity calculations were performed using the MTrackJ plugin in Fiji as described previously (26). For each tracked cell, average cell velocities from the first 70-hour period (pretreatment) and the second 70-hour period (treatment) were represented as paired measurements. In Supplementary Fig. S3, the migration distance of disseminated cells was measured as the direct line between the cell and the closest point on the organoid periphery at the endpoint (96 hours).

Tumor organoid invasion and dissemination

DIC images of human and murine tumor organoids cultured in 3D fibrillar collagen I were acquired on days 3 or 4 of culture. Organoids were scored as invasive if they had 2 or more strands of cells migrating into the 3D collagen matrix. Organoids were scored as disseminative if they had 3 or more disseminating cells in the field of view.

Published OnlineFirst November 1, 2019; DOI: 10.1158/0008-5472.CAN-18-3241

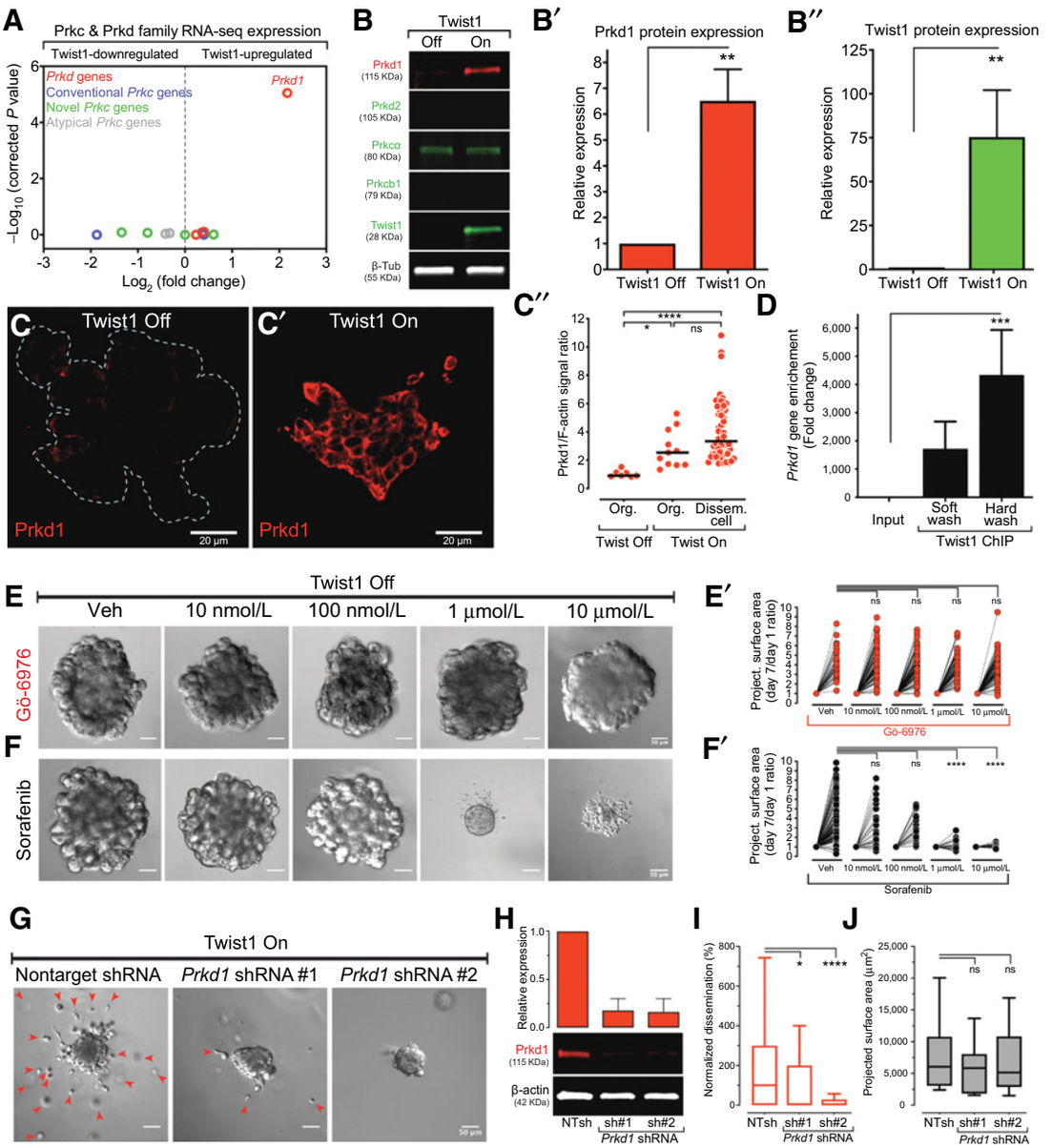

Figure 2.

Prkd1 is selectively required in Twist1-induced dissemination. **A,** Volcano plot showing differential expression of *Prkc* and *Prkd* gene family members in Twist1-On relative to Twist1-Off organoids (from dataset shown in **Fig. 1A** and previously published in ref. 5). **B,** Western blots showing Prkd1, Prkd2, Prkca, Pkrcb1, Twist1, and β-tubulin protein expression in Twist1-Off and Twist1-On organoids. **B′** and **B″,** Bar graphs (mean ± SEM) showing protein expression fold change for Prkd1 ($n = 5$ mice) and Twist1 ($n = 6$ mice), respectively, in Twist1-Off and Twist1-On organoids. Statistical test: Mann–Whitney. **, $P < 0.01$. **C** and **C′,** Confocal micrographs of Prkd1 immunofluorescence staining in Twist1-Off and Twist1-On organoids, respectively. Scale bar, 20 μm. **C″,** Dot plot (with median) showing Prkd1 expression levels in Twist1-Off organoids, and Twist1-On organoids and disseminated cells. For Twist1-Off, $r = 2$ mice; $n = 3$ organoids. For Twist1-On, $r = 2$ mice; $n = 11$ organoids (52 disseminated cells). Statistical test: Kruskal–Wallis. *, $P < 0.01$; ****, $P < 0.0001$. **D,** Bar graph (mean ± SEM) showing enrichment of Twist1 ChIP region in the *Prkd1* gene quantified using qPCR. Data are represented as fold change over input (non-IP) control. **E** and **F,** DIC micrographs of Twist1-Off organoids cultured for 7 days and treated with different doses of Gö-6976 or sorafenib. Scale bars, 50 μm. **E′** and **F′,** Paired dot plots showing fold change in projected surface area of organoids in **E** and **F**, respectively. For each drug, $r = 3$ mice; $n = 25$–105 organoids per dose. Statistical test: Kruskal–Wallis. ns, nonsignificant, $P > 0.05$; ****, $P < 0.0001$. **G,** DIC micrographs of Twist1-On organoids lentivirally transduced with nontarget (NT, control) shRNA and *Prkd1* shRNA clones #1 or #2. Red arrowheads, disseminated cells. Scale bar, 50 μm. **H,** Western blot and bar graph (mean ± SEM) showing Prkd1 protein expression in control (NT) or Prkd1 knockdown (sh#1, sh#2) Twist1-On organoids represented in **G**. Data are collected from $r = 2$ experiments. **I,** Whisker plot (Tukey method) showing dissemination in control (NT) or Prkd1 knockdown (sh#1, sh#2) Twist1-On organoids represented in **G**. Data are collected from $r = 3$ mice; $n = 65$ organoids (NT), 39 organoids (sh#1), 22 organoids (sh#2). Statistical test: Kruskal–Wallis. *, $P < 0.05$; ****, $P < 0.0001$. **J,** Whisker plot (10th–90th percentile) showing projected organoid surface area in control (NT) or knockdown (sh#1, sh#2) Twist1-On organoids represented in **G**. Data collected from $r = 3$ mice; $n = 20$ organoids (NT), 14 organoids (sh#1), 17 organoids (sh#2) Statistical test: Kruskal–Wallis. ns, nonsignificant, $P > 0.05$.

Published OnlineFirst November 1, 2019; DOI: 10.1158/0008-5472.CAN-18-3241

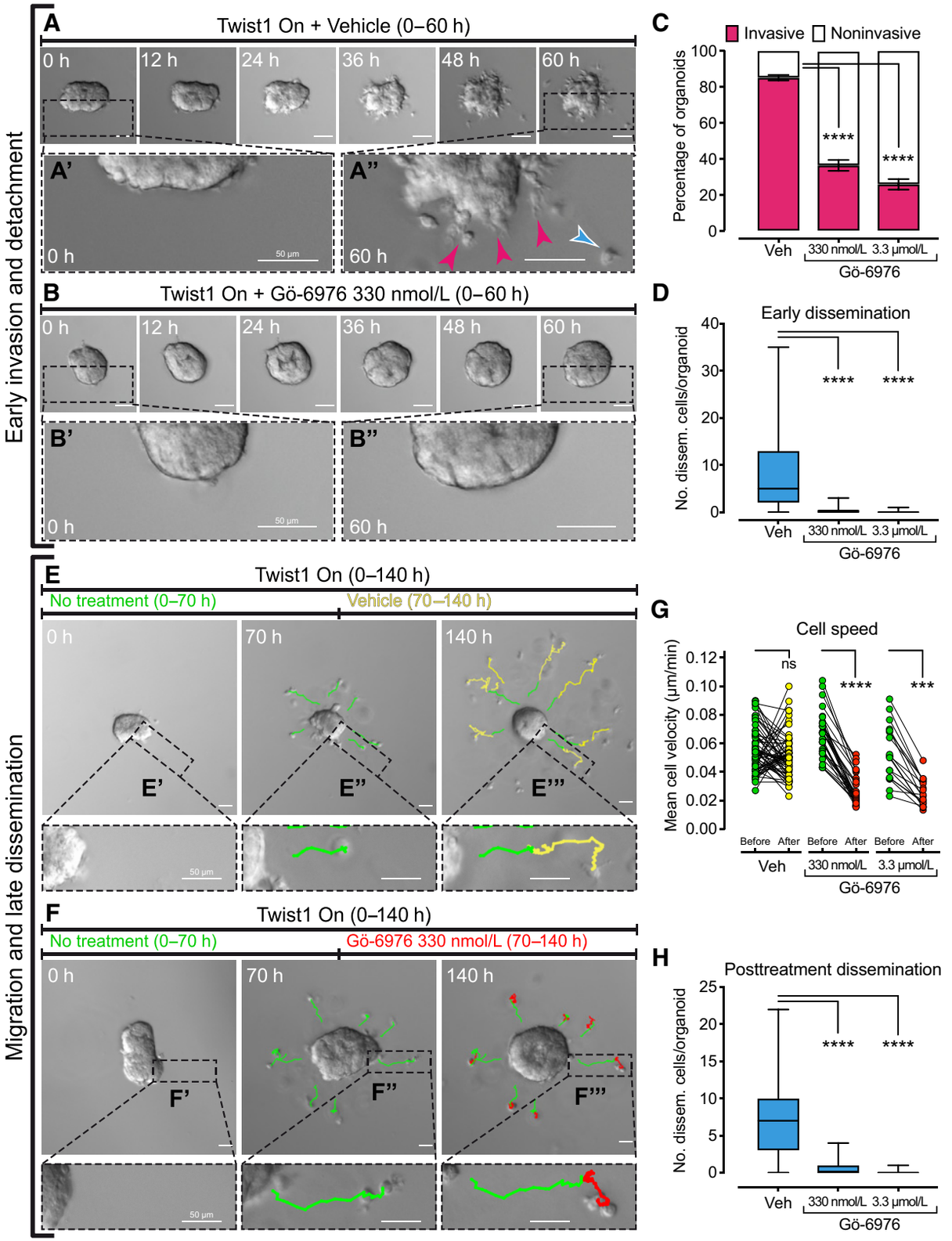

Published OnlineFirst November 1, 2019; DOI: 10.1158/0008-5472.CAN-18-3241

Western blotting

Organoids were extracted from 3D Matrigel by pipetting in cold PBS-EDTA buffer, comprised of: PBS (Life Technologies 10010-023), 20 mmol/L ethylenediaminetetraacetic acid (EDTA), and 1× protease inhibitor cocktail (Sigma-Aldrich 11873580001). The solubilized matrix–organoid mix was centrifuged for 5 minutes at 400 × *g*, 4°C, then washed twice by resuspension in cold PBS-EDTA and centrifuged for 5 minutes at 400 × *g*, 4°C. Cell lysis was performed in RIPA buffer (Millipore 20-188) with 5% glycerol, 0.2% SDS, and protease inhibitor cocktail. Electrophoresis, transfer, immunodetection, and scanning were performed using the Mini-Protean system (Bio-Rad 1658004) and Li-cor Fluorescence Odyssey System (Li-cor). Protein quantification was done in Fiji. Full blots are provided as a Supplementary File. Primary antibodies are listed in Supplementary Table S2.

Chromatin immunoprecipitation PCR

Genomic DNA was isolated from Twist1-On organoids, crosslinked, fragmented, and reverse-crosslinked using the truChIP Ultra-Low Chromatin Shearing Kit (Covaris PN520158), following the manufacturer's protocol. Immunoprecipitation and chromatin enrichment were performed per the Furlong lab protocol (http://furlonglab.embl.de/labData/protocols/ChIP-Seq.pdf). Two washing conditions, soft wash (without LiCl buffer) and hard wash (with LiCL buffer), were used to detect enrichment of Twist1-bound fragments. qPCR was performed using primers CTCACTAGGTCTTACTGTGTTGATA (forward) and TGTCTGGCTGGAGGTTTG (reverse) flanking a double E-box motif (CannTGnnnnnCAnnTG) in the *Prkd1* gene.

Lentiviral transduction

On day 0, 800 organoids were suspended in 50 μL organoid media including 3 μL of Viromag R/L magnetic particles (OZ Biosciences RL40200) and an adequate volume of viral particles for transduction at a multiplicity of infection of 8 viral particles per cell. The organoid–virus mix was then seeded in one well of cell-repellent 96-well plates (Greiner Bio-One 655970) and left to rest on top of a magnetic plate (OZ Biosciences, MF10000) for 2 hours at 37°C, 5% CO_2. Organoids were then incubated overnight at 37°C, 5% CO_2. On day 1, organoids were washed twice with organoid medium and incubated for 2 days. On day 3, culture medium was replenished and puromycin (2 μg/mL) was added for selection. On day 7, infected organoids were separated from single/dead cells using differential centrifugation (400 × *g*, 3 seconds, room temperature), embedded in 3D Matrigel (see previous section), and induced to express Twist1 with doxycycline-supplemented organoid media for 7 days.

Phospho-antibody microarray

Twist1-inducible organoids were collected from four 9.4-week-old littermates and cultured in 3D Matrigel for 5 days in 4 parallel experimental conditions: (i) Twist1-Off treated with vehicle control (DMSO); (ii) Twist1-On treated with vehicle control; (iii) Twist1-On treated with 1 μmol/L kb-NB142-70; (iv) Twist1-On treated with 1 μmol/L Gö-6976. Organoid media with vehicle, drug, and/or doxycycline were replenished every 48 hours. On day 5, organoids were extracted from Matrigel and lysed in ice-cold Kinexus Lysis Buffer (Kinexus Bioinformatics Corporation) supplemented with protease inhibitor cocktail (Sigma-Aldrich 11873580001) and PhosSTOP (Sigma-Aldrich 4906845001). Total protein extract from each sample was then chemically cleaved; protein was labeled with a fluorescent dye and then run on Kinexus KAM-880 Antibody Microarray (Kinexus, KAM-880 Kit) chips following the manufacturer's protocol. For analysis, individual phospho-antibody signal from each antibody spot was normalized to the intrasample median (for global signal normalization/chip) and to intersample average (to allow comparison of a specific phosphorylation between samples; Supplementary Table S3). After normalization, and to identify the set of phosphorylation upregulated in Twist1-On organoids but downregulated by either of the Prkd1 inhibitors, the following cutoff was applied for each phospho antibody: Intersample SD > 1.15, and fold change (Twist1-On/any other sample) > 0.1. At this cutoff, 81 protein phosphorylations were identified out of 359 total phosphorylations probed (Supplementary Table S3). Graphic representation of the data was generated using Prism 7 (GraphPad).

Gene coexpression in human breast tumors

TWIST1 and *PRKD1* mRNA coexpression analysis was assayed using the Targeted Correlation module in bc-GenExMiner v4.2 (http://bcgenex.centregauducheau.fr/BC-GEM/GEM-Accueil.php?js=1).

Patient distant metastasis-free survival

To obtain distant metastasis-free survival (DMFS) based on *TWIST1* and *PRKD1* mRNA expression (from gene chip microarrays) in patients with breast cancer, we utilized the open-source database Kaplan–Meier Plotter (kmplot.com). The following search parameters were applied: Survival, DMFS; User selected probe set, only JetSet; Auto selected best cutoff, yes; Use earlier release of the database, all; Use following dataset for the analysis: all. For the basal breast cancer population, we utilized the search parameter: Intrinsic subtype, basal.

Orthotopic transplantation of C3(1)-TAg organoids and analysis of tumor invasion and metastasis *in vivo*

Organoids from C3(1)-TAg;mTmG tumors were transduced with Prkd1 or control (nontarget) shRNA lentivectors, as described in the lentiviral transduction section. Fifty organoids were resuspended in 40 μL of a 50:50 DMEM:Matrigel solution and transplanted orthotopically into 3-week-old, female, NSG mice in a sterile hood. Host mice were anesthetized with 2.5% isoflurane and

Figure 3.

Prkd1 expression and activity are required for epithelial invasion, loss of cell-cell adhesion, and persistent migration. **A** and **B,** DIC micrographs from time-lapse imaging of Twist1-On organoids treated with vehicle (**A**) or Gö-6976 (**B**). Zoomed insets are presented for **A** in **A′** and **A″** and for **B** in **B′** and **B″**. Magenta and cyan arrowheads indicate ECM-invading cells and early disseminated cells, respectively. Scale bars, 50 μm. **C,** Stacked bar graph (mean with 95% confidence interval) showing quantification of the percentage of organoids with (magenta) or without (white) ECM-invading cells from **A** and **B**. **D,** Whisker plot (min to max) showing quantification of the number of disseminated cells per organoid from time-lapse movies represented in **A** and **B**. Data for **C** and **D** were collected from $r = 3$ mice, $n = 47$ (Veh), 33 (Gö-6976, 330 nmol/L), 31 (Gö-6976, 3.3 μmol/L) organoids. **E** and **F,** DIC micrographs and zoomed insets from time-lapse imaging of Twist-induced organoids during a 70-hour interval without treatment (**E′** and **E″**; **F′** and **F″**), then a 70-hour interval with treatment with vehicle (**E″** and **E‴**) or Gö-6976 (**F″** and **F‴**). Green, complete cell migration tracks for the 70-hour untreated phase. Full cell migration tracks for the 70-hour vehicle-treated or Gö-6976–treated phase are represented in yellow and red, respectively. Scale bars, 50 μm. **G,** Paired dot plot showing mean cell velocities of individual disseminating cells before or after treatment with vehicle or Gö-6976, for data represented in **E** and **F**. Data were collected from $r = 3$ mice, $n = 60$ cells (Veh), 30 cells (330 nmol/L), 18 cells (3.3 μmol/L). Statistical test: Kruskal–Wallis. ns, nonsignificant, $P > 0.05$; ***, $P < 0.001$; ****, $P < 0.0001$. **H,** Whisker plot (min–max) showing quantification of the number of disseminated cells per organoid in the 70-hour interval following treatment with vehicle or Gö-6976 (**F′** and **F″**). Statistical test: Kruskal-Wallis. ****, $P < 0.0001$.

Published OnlineFirst November 1, 2019; DOI: 10.1158/0008-5472.CAN-18-3241

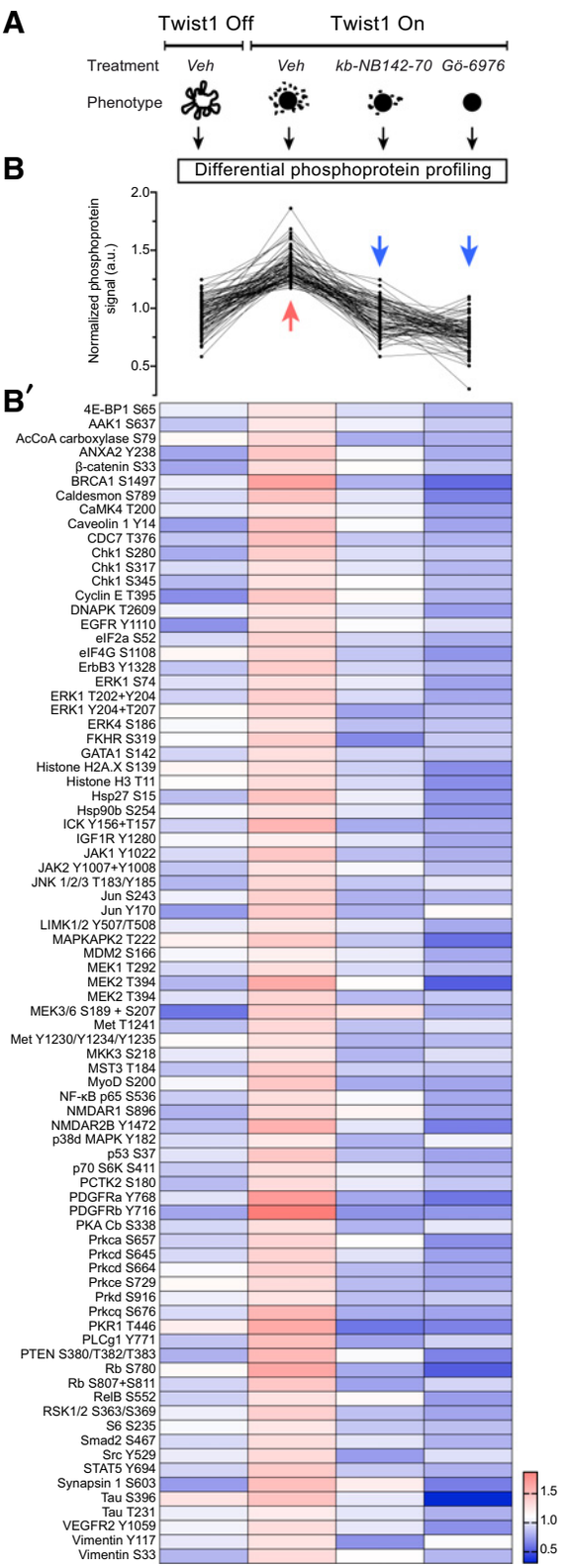

immobilized on a sterile surface. On each side of the mouse, the #4 mammary glands were exposed by two small incisions and the gland's lymph-proximal side was excised. Approximately 50 organoids (in 40 μL) were loaded into a microsyringe (Hamilton, 702RN-7636-01) and injected per residual gland on each side. The wounds received bupivicaine (Sigma, B5274), were closed using autoclips (BD Biosciences, 427631), and then treated with triple antibiotic ointment. Primary tumors and lungs were harvested 6 to 8 weeks posttransplantation, when maximum tumor diameter reached 20 mm. Primary mammary tumors were sectioned, stained with DAPI or anti-Twist1, and scanned using the Axio Scan.Z1 microscope (Zeiss) to assess invasion. Lungs were examined for metastases under the dissection microscope using lentiviral eGFP fluorescence and representative images were acquired with an iPhone XS. GFP^+ foci were counted as metastases using ImageJ.

Statistical analysis

Statistical analysis was performed and graphs were plotted in Prism 7 (GraphPad). We utilized the D'Agostino–Pearson omnibus test to assess normality. When data were not normally distributed, we used the two-tailed Mann–Whitney test to compare two datasets, or the Kruskal–Wallis test (with Dunn correction for multiple comparisons) to compare three or more datasets. Statistical significance was considered starting from $P < 0.05$. The underlying data used to generate quantitative elements of the figures are provided at the following link: https://github.com/EwaldLab/2019_Prkd1/.

Additional materials, instrumentation, and methods pertaining to microscopy and constructs are detailed in Supplementary Methods.

Results

Identifying targetable molecular effectors of Twist1-induced dissemination

We first tested the requirement for genes upregulated by Twist1 during dissemination, based on previous RNA-seq profiling of Twist1-On versus Twist1-Off mammary organoids (106 transcripts; CMV::rtTA-TetO::Twist1 mouse; ref. 5). From this list, we identified 8 genes (Prkd1, Tgfbr2, Dusp1, Sphk1, Cxcl12, Ccl2, Mme, Cacna1c) for which small-molecule inhibitors or receptor antagonists were available (**Fig. 1A**; Supplementary Table S1). In addition to RNA-seq–predicted inhibitors (**Fig. 1B**, red symbols), we tested inhibitors of matrix degradation (Batimastat, GM6001; ref. 6), adhesion (RGD peptide), cell proliferation (aphidicolin; ref. 6), clinically approved drugs (sorafenib, taxol), and inhibitors for the off-targets (JAK, Trk, Prkc) of Twist1-predicted drugs (**Fig. 1B**, black symbols; Supplementary Table S1). For each compound, we characterized the dose dependence of inhibition of dissemination in 3D-cultured Twist1-On organoids. Dissemination was visualized using differential

Figure 4.

Identification of Twist1-upregulated and Prkd1-maintained phosphorylations in disseminating organoids. **A,** Experimental outline showing Twist1-inducible organoids utilized for phospho-antibody microarray. Four culture conditions were tested: Twist1-Off vehicle-treated organoids (undergo branching morphogenesis), Twist1-On organoids (undergo dissemination), and Twist1-On organoids treated with either kb-NB142-70 (1 μmol/L) or Gö-6976 (1 μmol/L; dissemination inhibited). **B,** Linear plot showing 81 protein phosphorylations (out of 359 tested) identified by phospho-antibody microarray to be increased in Twist1-On compared with Twist1-Off organoids (red arrow) and decreased in Prkd1-inhibited compared with vehicle-treated Twist1-On organoids (blue arrows). **B′,** Heatmap of the protein phosphorylations identified in **B**. Color scale bar, fold change.

Published OnlineFirst November 1, 2019; DOI: 10.1158/0008-5472.CAN-18-3241

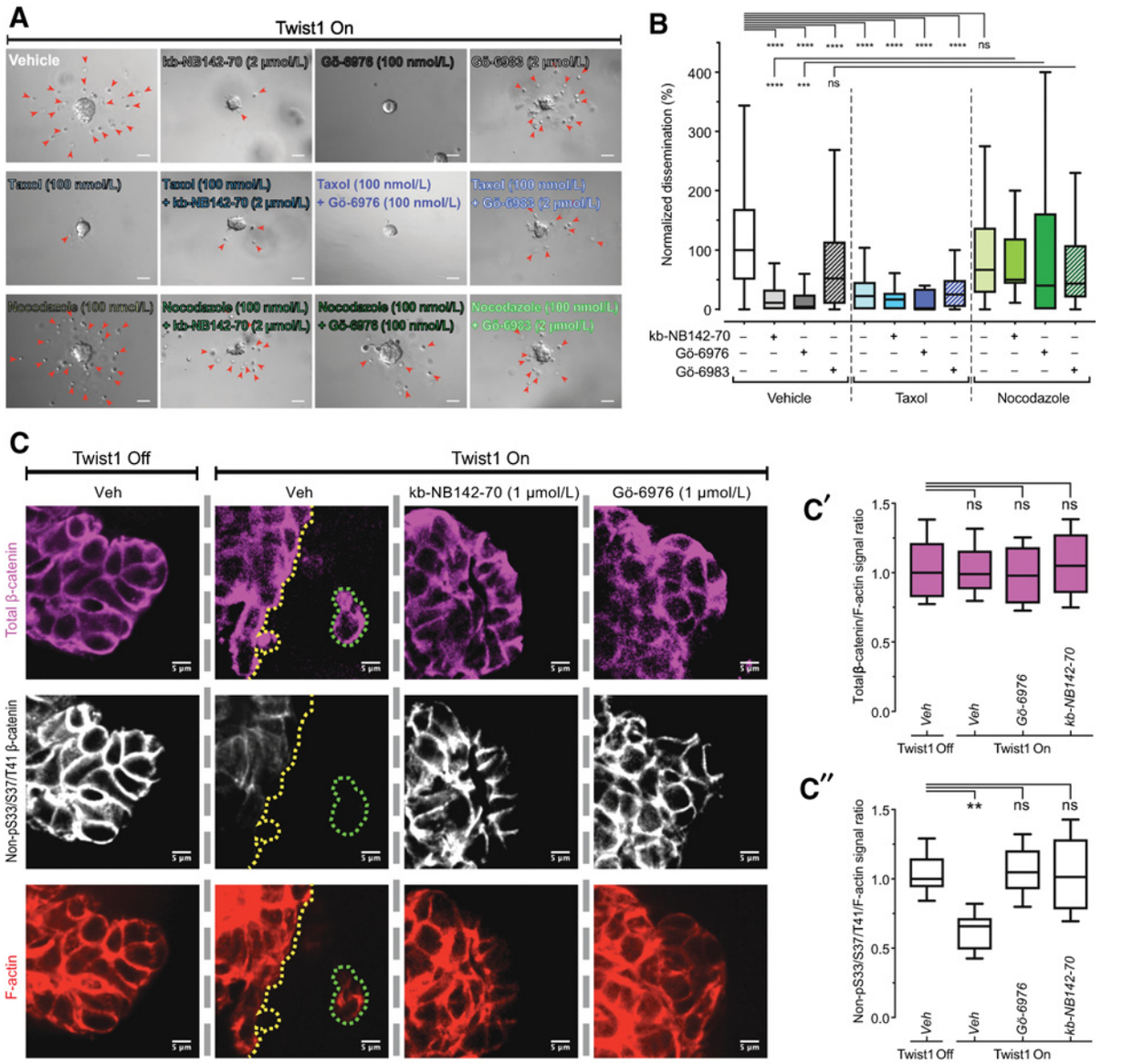

Figure 5.

Twist1 induces Prkd1-dependent phosphorylation of Tau and β-catenin. **A,** DIC micrographs of Twist1-On organoids treated with vehicle, Gö-6976, kb-NB142-70, and Gö-6983, taxol, and nocodazole alone or in combinations (as specified). Red arrowheads, disseminated cells. Scale bars, 100 μm. **B,** Whisker plot (Tukey method) showing dissemination quantification of Twist1-On organoids represented in **A**. Data are collected from $r = 3$ mice, $n = 581$ (Veh), and 38-155 organoids (drug treatment). Statistical test: Kruskal–Wallis. ns, nonsignificant, $P > 0.05$; ***, $P < 0.001$; ****, $P < 0.0001$. **C,** Confocal micrographs of fluorescently labeled total β-catenin (magenta), nonphosphorylated S33/S37/T41 (non-pS33/S37/T41) β-catenin (white), and F-actin (red) in organoids treated as indicated in **A**. Dotted lines outline organoid-matrix border (yellow), or disseminated cell contour (green). Scale bars, 5 μm. **C′** and **C″,** Whisker plots (min–max) showing relative fluorescence intensity of total β-catenin (**C′**) and non-pS33/S37/T41 β-catenin (**C″**) from micrographs represented in **C**. Data are collected from $n = 3$ mice, $r = 6$–8 organoids per condition. Statistical test: Kruskal–Wallis. ns, nonsignificant, $P > 0.05$; **, $P < 0.01$.

interference contrast (DIC) microscopy and we calculated both the IC_{50} and the dissemination level at 1 μmol/L, normalized to vehicle control (**Fig. 1B**). Two clinically approved drugs (sorafenib, taxol), and three RNA-seq–predicted compounds (targeting Prkd1 or TGFβR-2) were potent inhibitors of dissemination, with an $IC_{50} < 1$ μmol/L and dissemination at 1 μmol/L < 33.3% (**Fig. 1B′**). These results reveal that Prkd1 and TGFβ signaling are targetable and essential effectors of Twist1-induced dissemination.

TGFβ signaling is known to induce EMT (27, 28) and its identification validates our approach. Consistent with the cooperative requirement for TGFβR-1 and -2 (27, 28), treatment with a TGFβR-1 inhibitor phenocopied the TGFβR1/2 inhibitor (**Fig. 1B**). We next stimulated TGFβ signaling by treating organoids with recombinant TGFβ1. TGFβ1 addition prevented branching morphogenesis but did not induce dissemination in Twist1-Off organoids; in contrast, TGFβ1 increased dissemination of Twist1-On organoids

Published OnlineFirst November 1, 2019; DOI: 10.1158/0008-5472.CAN-18-3241

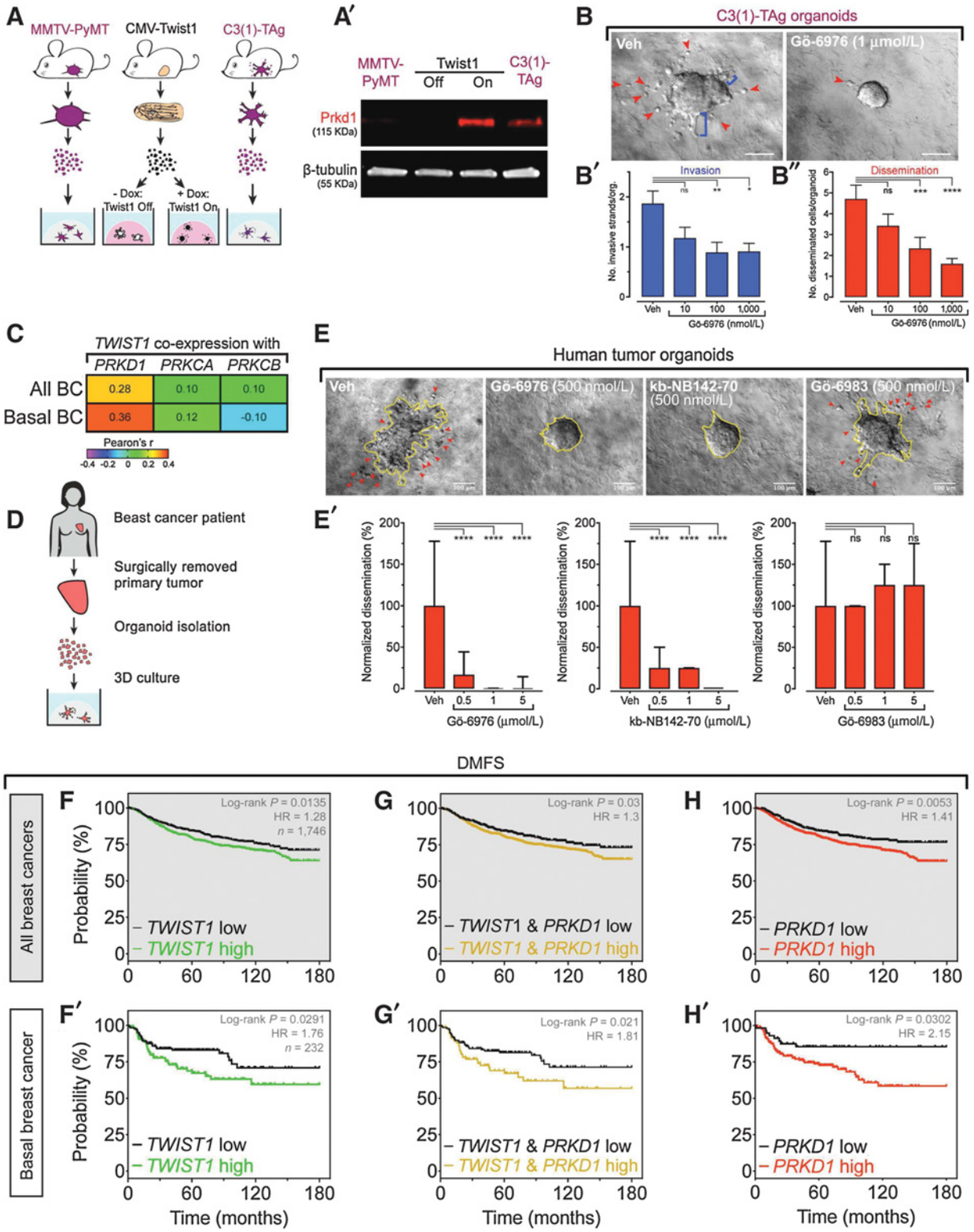

Figure 6.

Prkd1 is required for mammary tumor organoid invasion and correlates with metastatic outcome in patients. **A,** Experimental outline for mammary organoid culture from the Twist1-inducible model and the two breast cancer models MMTV-PyMT and C3(1)-TAg. **A′,** Western blots showing Prkd1 protein expression (and β-tubulin as a control) in organoids from mouse models shown in **A**. **B,** DIC micrographs showing C3(1)-TAg tumor organoids treated with vehicle or Gö-6976 (1 μmol/L). Blue brackets, invasion strands; red arrowheads, disseminated cells. Scale bars, 100 μm. (*Continued on the following page.*)

Published OnlineFirst November 1, 2019; DOI: 10.1158/0008-5472.CAN-18-3241

without reducing protein levels of E-cadherin, β-catenin, or αE-catenin (Supplementary Fig. S1A–S1G). We conclude that Twist1-induced dissemination requires downstream TGFβ signaling and that combined stimulation with Twist1 and TGFβ1 is not sufficient to eliminate epithelial gene expression in primary mammary cells.

The two lowest IC_{50}s in our dissemination assay corresponded to inhibitors of Prkd1: kb-NB142-70 (IC_{50} = 106.9 nmol/L, dissemination at 1 μmol/L = 31%), which targets Prkd1/2/3 (29) and Gö-6976 (IC_{50} = 11.49 nmol/L, dissemination at 1 μmol/L = 0%), which targets Prkca/Prkcb1/Prkd1 (**Fig. 1B**; Supplementary Fig. S2A and S2B'; refs. 30, 31). As Gö-6976 affects Prkc in addition to Prkd, we assayed two more selective Prkc inhibitors, Gö-6983 and Ro 32-0432 hydrochloride, and observed minimal effects on dissemination (Gö-6983: IC_{50} 1043 nmol/L, dissemination at 1 μmol/L 52.2%; Ro 32-0432 hydrochloride: no inhibition, curve fit was not possible; **Fig. 1B**). These data suggest that Prkd1, not Prkc, is the critical target of Gö-6976 and kb-NB142-70 in Twist1-On organoids, and that Prkc signaling is not essential for Twist1-induced dissemination. However, effectively inhibiting dissemination by targeting Prkd1 requires potent inhibitors with low *in vitro* IC_{50}s as CID-755673, a weak inhibitor with reported 9.1- and 6.5-fold lower *in vitro* IC_{50}s compared with Gö-6976 and kb-NB142-70, respectively (29, 32), did not affect dissemination. Furthermore, inhibition of Prkd2 and Prkd3 (but not Prkd1) by CID-2011756 (33) did not affect dissemination, supporting the concept that the effect of Gö-6976 is through selective inhibition of Prkd1 (**Fig. 1B**). Taken together, our results suggest that Prkd1 is a required effector of Twist1-induced dissemination and that its targeting requires potent selective inhibitors such as Gö-6976 and kb-NB142-70.

Prkd1 is the only Prkc/Prkd gene differentially expressed and it is required for Twist1-induced dissemination

We next assayed for differential expression of Prkc and Prkd gene family members in Twist1-On versus Twist1-Off organoids and observed that Twist1 induced Prkd1 expression at RNA (**Fig. 2A**) and protein (**Fig. 2B–B″**) levels. Other Prkd or Prkc genes were not differentially expressed by Twist1 (**Fig. 2A** and **B**). Immunofluorescence revealed increased protein levels and chiefly membrane localization of Prkd1 protein in Twist1^{+} cells (**Fig. 2C–C″**). We next used chromatin immunoprecipitation (ChIP) with an anti-Twist1 antibody followed by qPCR to establish that Twist1 protein directly binds the *Prkd1* gene (**Fig. 2D**). Normal mammary organoids do not express Prkd1 and treatment with Gö-6976 did not significantly affect their growth or branching morphogenesis (**Fig. 2C, E** and **E′**). In contrast, normal organoids treated with sorafenib exhibited significant growth inhibition starting from 1 μmol/L (**Fig. 2F** and **F′**). Finally, we tested whether shRNA knockdown of *Prkd1* would phenocopy Gö-6976 treatment. Transduction of Twist1-On organoids with lentiviral shRNA targeting *Prkd1* significantly reduced dissemination (**Fig. 2G–I**) without affecting growth (**Fig. 2G** and **J**). Our findings reveal that Prkd1 is directly and selectively induced by Twist1, is required for dissemination, and can be pharmacologically targeted with minimal effect on normal cells.

Prkd1 is required for invasion, loss of adhesion, and migration

We next evaluated the temporal requirement for Prkd1 by imaging Twist1-On organoids while inhibiting Prkd1 either simultaneously with (**Fig. 3A–D**) or 70 hours after (**Fig. 3E–H**) Twist1 induction with doxycycline. Twist1 induction led to invasive phenotypes (defined as the presence of ECM-directed protrusions and disseminated cells) in 85% of vehicle-treated organoids, while treatment with Gö-6976 at 330 nmol/L or 3.3 μmol/L reduced the frequency of invasive phenotypes to 36% and 25%, respectively, and completely blocked cell detachment (**Fig. 3A–D**; Supplementary Movie S1). We conclude that both initial ECM invasion and loss of cell–cell adhesion require Prkd1 activity.

We next tested the requirement for Prkd1 for migration by tracking the motility of disseminated single cells before and after treatment with vehicle or Gö-6976 (**Fig. 3E–H**). Vehicle treatment did not alter migration speed, while treatment with Gö-6976 abrogated cell motility (**Fig. 3E–F‴** and **G**; Supplementary Movie S2). We observed an analogous reduction in disseminated cell displacement in *Prkd1*-knockdown organoids (Supplementary Fig. S3A–S3A′). Prkd1 activity is, therefore, also required to sustain cell migration after dissemination. Furthermore, treatment with Gö-6976 significantly reduced new dissemination events at late timepoints, relative to vehicle control (**Fig. 3H**).

Identification of downstream effectors of Prkd1 phosphosignaling during dissemination

We then tested the requirement for Prkd1's kinase activity by overexpressing a kinase-dead mutant (K612W; ref. 34). We observed a significant reduction of dissemination, suggesting that this construct acts as a dominant negative and that Prkd1 kinase activity is required (Supplementary Fig. S3B and S3B′). We next sought to identify Prkd1's signaling consequences systematically using antibody microarrays measuring phospho-protein levels. We compared the following conditions: Twist1-Off (Prkd1 not detectable), Twist1-On (Prkd1 expressed), and Twist1-On treated with either kb-NB142-70 or Gö-6976 (Prkd1 expressed and inhibited; (**Fig. 4A**). We identified 81 protein phosphorylations that increased when Prkd1 was active and decreased when Prkd1 was inhibited (**Fig. 4B**, red vs. blue arrows). Among these were several regulators of tumor progression (e.g., Brca, PTEN, Rb, p53, VEGFR, EGFR, Met) as well as components of the MAP kinase (e.g., MEK1/2/4/6, ERK1/4, Erb3, MKK3, p38d, MAPKAPK2, JNK1/2/3, Jun, Rsk1/2) and NF-κB (e.g., p65, relB) pathways (**Fig. 4B′**).

Given that dissemination involves cytoskeletal remodeling, we focused on microtubule and actin-related proteins. There were two Prkd1-dependent phosphorylations on the microtubule-associated protein Tau (T231 and S396; **Fig. 4B′**), both of which can promote microtubule disassembly (35, 36). We therefore assessed the coregulation of Prkd1 and microtubule dynamics during dissemination. We treated Twist1-induced organoids with taxol (microtubule stabilizer) or nocodazole (microtubule destabilizer) in combination with either a Prkd1 inhibitor (Gö-6976 or kb-NB142-70) or a Prkc inhibitor (Gö-6983; **Fig. 5A** and **B**). Taxol alone significantly reduced dissemination compared with vehicle control, while Prkd1

(*Continued.*) **B′** and **B″,** Bar graphs (mean ± SEM) showing quantification of the number of invasive strands (**B′**) and disseminated cells (**B″**) per organoid. Data are collected from $r = 3$ mice; $n = 39–57$ organoids per dose. Statistical test: Kruskal–Wallis. ns, nonsignificant, $P > 0.05$; **, $P < 0.01$; ****, $P < 0.0001$. **C,** Heatmap showing mRNA coexpression of *TWIST1* with either *PRKD1, PRKCA*, or *PRKCB* in human breast tumors (data from bc-GenExMiner). The color scale indicates Pearson *r*, and the exact value is indicated in each box. **D,** Experimental outline for organotypic culture of surgically isolated human breast tumors. **E,** Representative DIC micrographs of human tumor organoids treated with Gö-6976, kb-NB142-70, or Gö-6983. Yellow outline, organoid. Red arrowheads, disseminated cells. Scale bar, 100 μm. **E′,** Bar graph (median ± interquartile range) showing quantified dissemination of human tumor organoids treated with increasing doses of drugs used in **E**. Statistical test: Kruskal–Wallis. ns, nonsignificant, $P > 0.05$; ****, $P < 0.0001$. **F–H,** Kaplan–Meier plots showing DMFS in a general population of 1,746 patients with breast cancer and in a subset of 232 patients with basal breast cancer (**F′**, **G′**, and **H′**). Patient groups were separated based on *TWIST1* and/or *PRKD1* mRNA expression.

Published OnlineFirst November 1, 2019; DOI: 10.1158/0008-5472.CAN-18-3241

inhibitors alone or in combination with taxol potently blocked dissemination (**Fig. 5A** and **B**). Treatment with nocodazole alone did not affect dissemination but, interestingly, combining nocodazole with a Prkd1 inhibitor partially rescued dissemination from the suppressive effects of Gö-6976 and kb-NB142-70 (**Fig. 5A** and **B**). However, combining nocodazole with Prkc inhibitor Gö-6983 did not modify the partial effect of Gö-6983 alone (**Fig. 5A** and **B**). Live/dead staining of treated organoids revealed >95% cell viability across all conditions, suggesting that the effects were target specific and not due to general toxicity (Supplementary Fig. S4A and S4B). Our data demonstrate a requirement for microtubule dynamics in Twist1-induced dissemination and suggest that microtubule instability is essential to the prodisseminative function of Prkd1.

To investigate whether Twist1 regulates the adherens junction, we focused on the Prkd1-dependent S33 phosphorylation of β-catenin (**Fig. 4B′**), a modification linked to its ubiquitination and degradation (37, 38). Immunofluorescence and Western blotting revealed that total β-catenin levels and localization were stable after Twist1 expression (Supplementary Figs. S1G and S5A–S5B). We next evaluated the subcellular localization of pS33 β-catenin via coimmunostaining for total and S33/S37/T41 nonphosphorylated β-catenin. In Twist1-Off organoids, total β-catenin and S33/S37/T41 nonphosphorylated β-catenin were both localized to the plasma membrane, suggesting a highly expressed and poorly phosphorylated β-catenin that is likely competent for cell adhesion (**Fig. 5C**). In Twist1-On organoids, total β-catenin remains membrane localized but S33/S37/T41 nonphosphorylated β-catenin signal decreased in the organoid bulk and disappeared in disseminated cells (**Fig. 5C–C″**). These staining patterns suggest a Twist1-dependent mechanism for release of cell–cell adhesion through β-catenin phosphorylation. Finally, inhibition of Prkd1 with kb-NB142-70 (1 μmol/L) or Gö-6976 (1 μmol/L) restored normal levels of non-pS33/S37/T41 β-catenin without affecting total β-catenin level (**Fig. 5C–C″**). We did not observe nuclear translocation of β-catenin in any condition. Our results reveal that S33 β-catenin phosphorylation is regulated by Twist1 expression and Prkd1 activity, and that it correlates with dissemination.

Prkd1 is required for tumor invasion and metastasis

To assess the role of Prkd1 in breast cancer, we assayed Prkd1 expression in genetically engineered mouse models of luminal, MMTV-PyMT (21), and basal, C3(1)-TAg, breast cancer (**Fig. 6A**; ref. 22). We focused on the C3(1)-TAg model, as MMTV-PyMT cells did not express Prkd1, while C3(1)-TAg cells express high levels of Prkd1 in culture and Twist1 *in vivo* (**Fig. 6A′**; Supplementary Fig. S6A). Treatment of C3(1)-TAg organoids with the Prkd1 inhibitor, Gö-6976, reduced the number of invasion strands and disseminated cells (**Fig. 6B–B‴**). The significance of Prkd1 in breast cancer was further supported by gene expression analysis in human tumors, which showed a strong correlation of *TWIST1* with *PRKD1* (but not *PRKCA* or *PRKCB*). This coexpression increases in basal breast cancer (**Fig. 6C**). This result prompted us to assay the impact of Prkd1 inhibition on the invasion and dissemination of freshly isolated primary human breast tumors organoids (**Fig. 6D**; ref. 2). Strikingly, Gö-6976 dose dependently decreased invasion and dissemination across organoids from 6 patients (Supplementary Fig. S6B–S6B″). We then compared the effect of equal doses of Gö-6976, kb-NB142-70, and Gö-6993 on organoids isolated from an independent cohort of 3 patients and found that only the Prkd1 inhibitors (Gö-6976 and kb-NB142-70) blocked dissemination (**Fig. 6E** and **E′**). These inhibitors did not cause significant toxicity in human tumor organoids (Supplementary Fig. S6C–S6C‴). Taken together, these results demonstrate that Prkd1 is selectively required for dissemination in human breast tumors. We next examined the correlation between DMFS of patients with breast cancer and their expression of *TWIST1* or *PRKD1*. In a cohort of 1,746 patients representing all types of breast cancers (dataset from KMplot.com), we found that high *TWIST1* and *PRKD1* mRNA expression associates with a statistically significant decrease in DMFS (**Fig. 6F–H**). In a cohort of patients with basal breast cancer, we found a stronger association with poor DMFS than in the general breast cancer population (**Fig. 6F′–H′**).

To assay the requirement for Prkd1 in local tumor invasion and distant metastasis in basal breast cancer *in vivo*, we knocked down *Prkd1* in C3(1)-TAg organoids and transplanted these into precleared fat pads of recipient NSG mice (**Fig. 7A** and **B**). We found that *Prkd1* knockdown reduced invasiveness at the tumor–stroma border (**Fig. 7C** and **D′**) and that Prkd1-knockdown tumors yielded significantly fewer lung metastases (**Fig. 7E–G**). Taken together, our findings support the conclusion that Prkd1 activity promotes cancer invasion and metastasis in a mouse model of basal breast cancer and that *PRKD1* expression correlates with poor outcomes in patients.

Discussion

We sought to identify the transcriptional and signaling mechanisms utilized during Twist1-induced epithelial dissemination. Starting from differential RNA-seq data (5), we tested the requirement for the protein products of eight genes that are transcriptionally upregulated by Twist1. Inhibitors of Cacna1c, Dusp1, Mme, Sphk1, and the chemokine receptors CXCR4 and CCR4 had little to no effect on dissemination. In contrast, inhibition of TGFβR1/2 or Prkd1 effectively inhibited dissemination. Given TGFβ's known role in dissemination (27, 28), its identification validates our approach. We focused on Prkd1 as its role downstream of Twist1 was not previously known. Prkd1 was the only member of the Prkc or Prkd families to be transcriptionally upregulated by Twist1 and we observed minimal effect from pharmacologic inhibition of Prkc, suggesting a selective role for Prkd1 during dissemination.

Once activated, Prkd1 regulates diverse cellular processes including gene expression, protein transport, apoptosis, proliferation, and cell motility (18). Among the phosphoregulated proteins downstream of Prkd1, we found regulators of tumor progression including Brca, PTEN, Rb, p53, VEGFR, EGFR, and Met. We also identified two Prkd1-dependent phosphorylations of Tau (T231 and S396) known for promoting microtubule depolymerization (35, 36), suggesting that Prkd1 can induce invasion by promoting microtubule instability. Consistent with this concept, stabilization of microtubules by taxol potently blocked dissemination and induction of microtubule instability by nocodazole partially rescued the effects of Prkd1 inhibition. Further supporting this link, prior studies found that microtubule depolymerization can activate Prkd1 (19, 20). Our data suggest that Prkd1 contributes to sustaining its own activation by promoting Tau phosphorylation (19, 20).

Twist1-induced cells disseminate while maintaining expression and membrane localization of E-cadherin, β-catenin, αE-catenin (5), raising the question of how they release from an epithelial tissue. A potential mechanism is suggested by our observation of a strong positive correlation between Prkd1 activity, phosphorylation of β-catenin at S33, and dissemination. Although β-catenin has previously been shown to be directly phosphorylated by Prkd1 on T112 and T120 (39), its phosphorylation on S33 is more likely mediated by GSK3-β (40). We also identified Prkd1-dependent phosphorylations

Published OnlineFirst November 1, 2019; DOI: 10.1158/0008-5472.CAN-18-3241

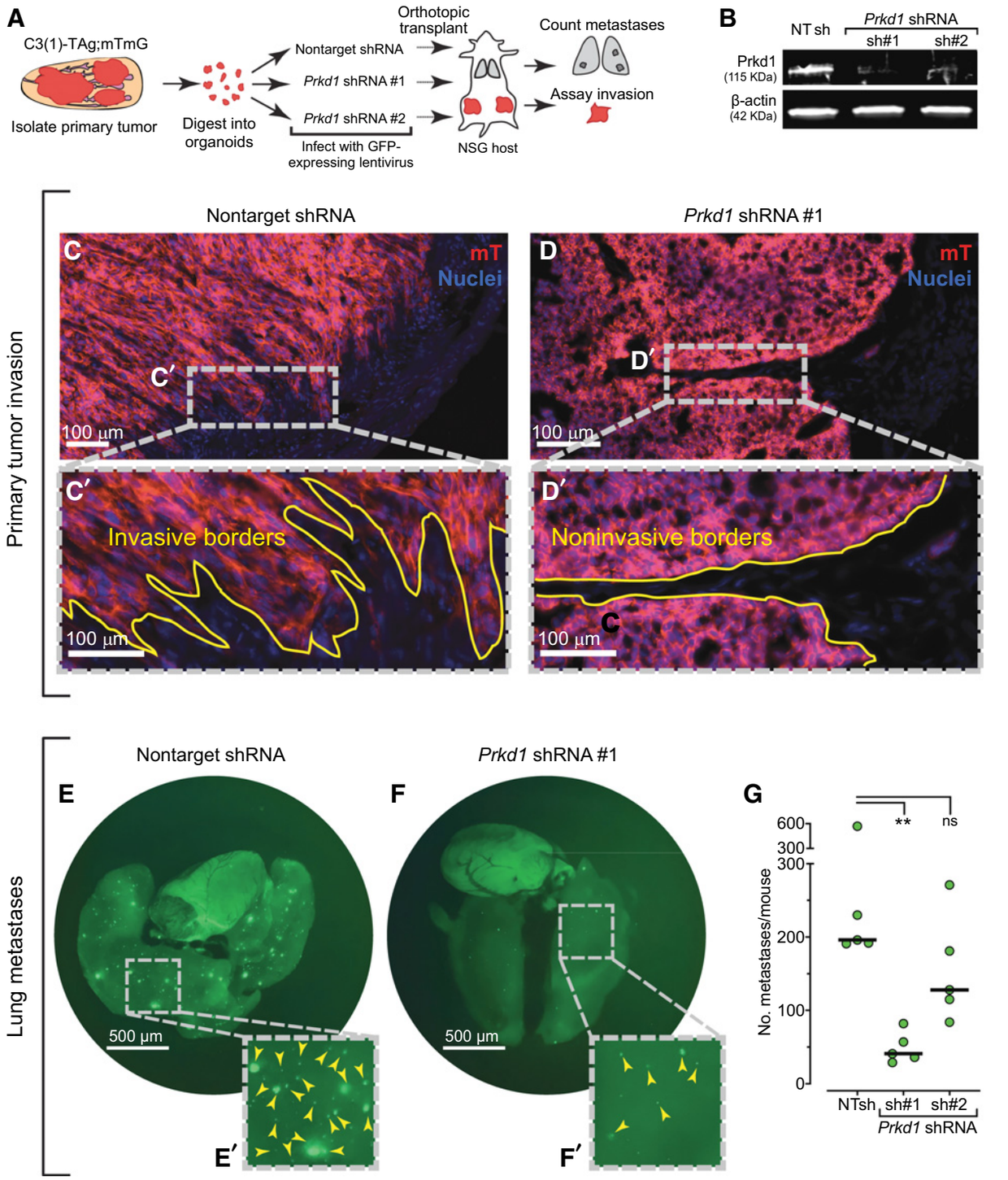

Figure 7.

Prkd1 is required for C3(1)-TAg tumor invasion and metastasis *in vivo*. **A,** Experimental outline for lentiviral shRNA transduction in C3(1)-TAg;mTmG tumor organoids followed by their transplantation into recipient NSG mice with precleared mammary fat pads. **B,** Western blot validating Prkd1 knockdown in C3(1)-TAg;mTmG tumor organoids prior to orthotopic transplantation. **C** and **D,** Micrographs of transplanted C3(1)-TAg;mTmG tumor cryosections from **A** with DAPI-stained nuclei (blue). Red, tumor cell membranes expressing mT (membrane Tomato). Scale bar, 100 μm. **C′** and **D′,** Zoomed insets of micrographs in **C** and **D** showing tumor-stroma border (yellow line). **E** and **F,** Macrographs of whole lungs of tumor-receiving mice, with GFP displaying metastatic colonies. Scale bar, 500 μm. **E′** and **F′,** Zoomed insets from **E** and **F,** with metastatic colonies indicated by yellow arrowheads. **G,** Dot plot (with median bar) showing the quantification of lung metastases as represented in **E** and **F**. **, $P < 0.01$.

Published OnlineFirst November 1, 2019; DOI: 10.1158/0008-5472.CAN-18-3241

on LIMK and Src, which could promote invasive motility. LIMK phosphorylation on T508 could be mediated by Rock and promote migration by local stimulation of the cofilin activation–inactivation cycle (41, 42). Src phosphorylation on Y529 primes its binding to integrins without activating integrin signaling (43), thus suggesting a stand-by role of integrin-mediated adhesion during Twist1-induced dissemination. Indeed, blocking integrin anchorage with soluble RGD peptide did not affect dissemination. In addition, matrix degradation assisted but was not required for Twist1-induced cells to disseminate (6). Collectively, these results suggest that Twist1 induces an amoeboid migration mode (44) in disseminating mammary epithelial cells.

EMT is a major model for dissemination and metastasis and so it is worth considering how our data fit with prior studies. Using 3D culture and *in vivo* methods based on EMT-dependent cell lines (e.g., MDA-MB-231, NMuMG), previous publications found an EMT-suppressing role of Prkd1 (45–47). Furthermore, possibly due to genetic drift or differences in experimental strategies, the same cell line yielded varied conclusions on the role of Prkd1 in tumor progression. For example, in MDA-MB-231 cells, Prkd1 was found to be promoting invadopodia formation (48) or suppressing invasion by preventing EMT (46). In MCF-7 cells, Prkd1 promoted (49) and inhibited (46) distinct aspects of tumor progression. These inconsistencies motivated investigators to ask how the anti-EMT, anti-invasive role of Prkd1 in breast cancer can be reconciled with its proinvasive role in other cancers (e.g., pancreatic and prostate; ref. 50). Our study identified a proinvasive, prodisseminative role for Prkd1 by using primary mammary organoids from a Twist1-expressing mouse model and by validating in both a metastatic mouse model for breast cancer and in primary patient tumor tissue.

We found that Prkd1 expression correlates with Twist1 expression and, consistent with prior work (51, 52), increased metastatic burden in patients. These correlations were more pronounced in the basal breast cancer subtype. In human tumor organoids, Prkd1 inhibition led to decreased invasion and dissemination. We then used a Twist1^{+}, Prkd1^{+} basal breast cancer model [C3(1)-Tag] to demonstrate a requirement for Prkd1 in invasion and dissemination in 3D culture and also during primary tumor invasion and distant metastasis *in vivo*. Our findings suggest a novel molecular framework whereby Twist1 directly drives the transcriptional upregulation of Prkd1, whose activity promotes ECM-directed invasion, loss of cell–cell adhesion, persistent migration, and metastasis, all without loss of epithelial identity (Supplementary Fig. S7). This framework is consistent with multiple clinical observations, including that the majority of breast cancers (invasive ductal carcinomas) invade and metastasize without loss of epithelial identity (7) and that circulating tumor cells can coexpress epithelial markers and Twist1 (9).

From a therapeutic perspective, we speculate that the antidisseminative effect of taxol in our dissemination assay can partially explain its clinical benefit in preventing metastatic recurrence. Indeed, combining taxol with nontaxane antimitotic drugs reduces distant disease recurrence in breast cancer patients (53) and overall disease recurrence, with increased benefit for hormone receptor–negative (54) and hormone receptor–negative/Her2-negative (55) patients. The genetic requirement for Prkd1 for tumor invasion and metastasis in the C3(1)-TAg model *in vivo* highlights the potential impact of targeting dissemination on metastasis. Future investigation of Prkd1 inhibitors *in vivo* will be needed to evaluate their therapeutic potential.

Disclosure of Potential Conflicts of Interest

K. Coutinho is an intern (patent law) at Buchanan Ingersoll & Rooney PC. A.J. Ewald's wife is the clinical lead, Early Stage Immuno-Oncology Portfolio at Immunocore and has ownership interests in it. A.J. Ewald and V. Padmanaban are listed as inventors on unlicensed patent applications related to biomarkers of invasion and to antibody therapies for cancer. No potential conflicts of interest were disclosed by the other authors.

Authors' Contributions

Conception and design: D. Georgess, A.J. Ewald
Development of methodology: D. Georgess, V. Padmanaban, K. Coutinho, N.M. Neumann
Acquisition of data (provided animals, acquired and managed patients, provided facilities, etc.): D. Georgess, V. Padmanaban, O.K. Sirka, K. Coutinho, A. Choi, G. Frid, T. Inoue
Analysis and interpretation of data (e.g., statistical analysis, biostatistics, computational analysis): D. Georgess, V. Padmanaban, O.K. Sirka, K. Coutinho, A. Choi, T. Inoue, A.J. Ewald
Writing, review, and/or revision of the manuscript: D. Georgess, V. Padmanaban, K. Coutinho, G. Frid, N.M. Neumann, A.J. Ewald
Administrative, technical, or material support (i.e., reporting or organizing data, constructing databases): D. Georgess, V. Padmanaban
Study supervision: D. Georgess, T. Inoue, A.J. Ewald

Acknowledgments

We would like to thank Dr. Timothy J. Mitchison (Harvard University) for thoughtful discussion on the role of microtubules in Prkd activation, Dr. Isaac S. Chan (JHU) for sharing clinical expertise on taxane therapeutics, Dr. Jin Zhu (JHU) for expert advice on qPCR, and Mr. Matthew Perrone and Dr. Joel S. Bader (JHU) for thoughtful discussion of the data and manuscript. D. Georgess was supported by a Postdoctoral Fellowship Grant from the Susan G. Komen Foundation (PDF15332336) and a research grant from the LAU SAS School Research and Development Council (SRDC-F-2018-145). A.J. Ewald received support for this project through grants from the Breast Cancer Research Foundation/Pink Agenda (BCRF-18-048), the Metastatic Breast Cancer Network, the Twisted Pink Foundation, Hope Scarves, and the NIH/NCI (U01CA217846, U54CA2101732, 3P30CA006973). K. Coutinho and V. Padmanaban were supported by the Isaac Morris Hay and Lucille Elizabeth Hay Fellowship. N.M. Neumann was supported by the NIH/NIGMS (3T32GM007309) and T. Inoue was supported by the NIH/NIGMS (GM123130).

The costs of publication of this article were defrayed in part by the payment of page charges. This article must therefore be hereby marked *advertisement* in accordance with 18 U.S.C. Section 1734 solely to indicate this fact.

Received October 16, 2018; revised August 2, 2019; accepted October 28, 2019; published first November 1, 2019.

References

1. Siegel RL, Miller KD, Jemal A. Cancer statistics, 2017. CA Cancer J Clin 2017;67:7–30.
2. Cheung KJ, Ewald AJ. Illuminating breast cancer invasion: diverse roles for cell-cell interactions. Curr Opin Cell Biol 2014;30C:99–111.
3. Shibue T, Weinberg RA. EMT, CSCs, and drug resistance: the mechanistic link and clinical implications. Nat Rev Clin Oncol 2017;14:611–29.
4. Yang J, Mani SA, Donaher JL, Ramaswamy S, Itzykson RA, Come C, et al. Twist, a master regulator of morphogenesis, plays an essential role in tumor metastasis. Cell 2004;117:927–39.
5. Shamir ER, Pappalardo E, Jorgens DM, Coutinho K, Tsai W-T, Aziz K, et al. Twist1-induced dissemination preserves epithelial identity and requires E-cadherin. J Cell Biol 2014;204:839–56.

6. Shamir ER, Coutinho K, Georgess D, Auer M, Ewald AJ. Twist1-positive epithelial cells retain adhesive and proliferative capacity throughout dissemination. Biol Open 2016;5:1216–28.
7. Atkins KA, Kong C. Practical breast pathology: a diagnostic approach: a volume in the pattern recognition series. Philadelphia: Elsevier Health Sciences; 2012.
8. Kowalski PJ, Rubin MA, Kleer CG. E-cadherin expression in primary carcinomas of the breast and its distant metastases. Breast Cancer Res 2003;5:R217–22.
9. Bredemeier M, Edimiris P, Mach P, Kubista M, Sjoback R, Rohlova E, et al. Gene expression signatures in circulating tumor cells correlate with response to therapy in metastatic breast cancer. Clin Chem 2017;63:1585–93.
10. Bulfoni M, Gerratana L, Del Ben F, Marzinotto S, Sorrentino M, Turetta M, et al. In patients with metastatic breast cancer the identification of circulating tumor cells in epithelial-to-mesenchymal transition is associated with a poor prognosis. Breast Cancer Res 2016;18:30.
11. Xu Y, Xu Y, Liao L, Zhou N, Theissen SM, Liao XH, et al. Inducible knockout of Twist1 in young and adult mice prolongs hair growth cycle and has mild effects on general health, supporting Twist1 as a preferential cancer target. Am J Pathol 2013;183:1281–92.
12. Martin TA, Goyal A, Watkins G, Jiang WG. Expression of the transcription factors snail, slug, and twist and their clinical significance in human breast cancer. Ann Surg Oncol 2005;12:488–96.
13. Mironchik Y, Winnard PT Jr, Vesuna F, Kato Y, Wildes F, Pathak AP, et al. Twist overexpression induces in vivo angiogenesis and correlates with chromosomal instability in breast cancer. Cancer Res 2005;65:10801–9.
14. Banerjee A, Wu ZS, Qian P, Kang J, Pandey V, Liu DX, et al. ARTEMIN synergizes with TWIST1 to promote metastasis and poor survival outcome in patients with ER negative mammary carcinoma. Breast Cancer Res 2011;13:R112.
15. Xu Y, Hu B, Qin L, Zhao L, Wang Q, Jiang J. SRC-1 and Twist1 expression positively correlates with a poor prognosis in human breast cancer. Int J Biol Sci 2014;10:396–403.
16. Riaz M, Sieuwerts AM, Look MP, Timmermans MA, Smid M, Foekens JA, et al. High TWIST1 mRNA expression is associated with poor prognosis in lymph node-negative and estrogen receptor-positive human breast cancer and is co-expressed with stromal as well as ECM related genes. Breast Cancer Res 2012;14:R123.
17. Johannes FJ, Prestle J, Eis S, Oberhagemann P, Pfizenmaier K. PKCu is a novel, atypical member of the protein kinase C family. J Biol Chem 1994;269:6140–8.
18. Steinberg SF. Regulation of protein kinase D1 activity. Mol Pharmacol 2012;81:284–91.
19. Eisler SA, Curado F, Link G, Schulz S, Noack M, Steinke M, et al. A Rho signaling network links microtubules to PKD controlled carrier transport to focal adhesions. Elife 2018;7. DOI: 10.7554/eLife.35907.
20. Franz-Wachtel M, Eisler SA, Krug K, Wahl S, Carpy A, Nordheim A, et al. Global detection of protein kinase D-dependent phosphorylation events in nocodazole-treated human cells. Mol Cell Proteomics 2012;11:160–70.
21. Guy CT, Cardiff RD, Muller WJ. Induction of mammary tumors by expression of polyomavirus middle T oncogene: a transgenic mouse model for metastatic disease. Mol Cell Biol 1992;12:954–61.
22. Maroulakou IG, Anver M, Garrett L, Green JE. Prostate and mammary adenocarcinoma in transgenic mice carrying a rat C3(1) simian virus 40 large tumor antigen fusion gene. Proc Natl Acad Sci U S A 1994;91:11236–40.
23. Muzumdar MD, Tasic B, Miyamichi K, Li L, Luo L. A global double-fluorescent Cre reporter mouse. Genesis 2007;45:593–605.
24. Nguyen-Ngoc KV, Shamir ER, Huebner RJ, Beck JN, Cheung KJ, Ewald AJ. 3D culture assays of murine mammary branching morphogenesis and epithelial invasion. Methods Mol Biol 2015;1189:135–62.
25. Cheung KJ, Gabrielson E, Werb Z, Ewald AJ. Collective invasion in breast cancer requires a conserved basal epithelial program. Cell 2013;155:1639–51.
26. Georgess D, Mazzorana M, Terrado J, Delprat C, Chamot C, Guasch RM, et al. Comparative transcriptomics reveals RhoE as a novel regulator of actin dynamics in bone-resorbing osteoclasts. Mol Biol Cell 2014;25:380–96.
27. Pickup M, Novitskiy S, Moses HL. The roles of TGFβ in the tumour microenvironment. Nat Rev Cancer 2013;13:788–99.
28. Giampieri S, Manning C, Hooper S, Jones L, Hill CS, Sahai E. Localized and reversible TGFβ signalling switches breast cancer cells from cohesive to single cell motility. Nat Cell Biol 2009;11:1287–96.
29. Lavalle CR, Bravo-Altamirano K, Giridhar KV, Chen J, Sharlow E, Lazo JS, et al. Novel protein kinase D inhibitors cause potent arrest in prostate cancer cell growth and motility. BMC Chem Biol 2010;10:5.
30. Gschwendt M, Dieterich S, Rennecke J, Kittstein W, Mueller HJ, Johannes FJ. Inhibition of protein kinase C mu by various inhibitors. Differentiation from protein kinase c isoenzymes. FEBS Lett 1996;392:77–80.
31. Martiny-Baron G, Kazanietz MG, Mischak H, Blumberg PM, Kochs G, Hug H, et al. Selective inhibition of protein kinase C isozymes by the indolocarbazole Go 6976. J Biol Chem 1993;268:9194–7.
32. Sharlow ER, Giridhar KV, LaValle CR, Chen J, Leimgruber S, Barrett R, et al. Potent and selective disruption of protein kinase D functionality by a benzoxoloazepinolone. J Biol Chem 2008;283:33516–26.
33. Sharlow ER, Mustata Wilson G, Close D, Leimgruber S, Tandon M, Reed RB, et al. Discovery of diverse small molecule chemotypes with cell-based PKD1 inhibitory activity. PLoS One 2011;6:e25134.
34. Storz P, Doppler H, Johannes FJ, Toker A. Tyrosine phosphorylation of protein kinase D in the pleckstrin homology domain leads to activation. J Biol Chem 2003;278:17969–76.
35. Iqbal K, Alonso AD, Gondal JA, Gong CX, Haque N, Khatoon S, et al. Mechanism of neurofibrillary degeneration and pharmacologic therapeutic approach. J Neural Transm Suppl 2000;59:213–22.
36. Evans DB, Rank KB, Bhattacharya K, Thomsen DR, Gurney ME, Sharma SK. Tau phosphorylation at serine 396 and serine 404 by human recombinant tau protein kinase II inhibits tau's ability to promote microtubule assembly. J Biol Chem 2000;275:24977–83.
37. Liu C, Li Y, Semenov M, Han C, Baeg GH, Tan Y, et al. Control of beta-catenin phosphorylation/degradation by a dual-kinase mechanism. Cell 2002;108:837–47.
38. Yost C, Torres M, Miller JR, Huang E, Kimelman D, Moon RT. The axis-inducing activity, stability, and subcellular distribution of beta-catenin is regulated in Xenopus embryos by glycogen synthase kinase 3. Genes Dev 1996;10:1443–54.
39. Du C, Jaggi M, Zhang C, Balaji KC. Protein kinase D1-mediated phosphorylation and subcellular localization of beta-catenin. Cancer Res 2009;69:1117–24.
40. Sadot E, Conacci-Sorrell M, Zhurinsky J, Shnizer D, Lando Z, Zharhary D, et al. Regulation of S33/S37 phosphorylated beta-catenin in normal and transformed cells. J Cell Sci 2002;115:2771–80.
41. Bravo-Cordero JJ, Magalhaes MA, Eddy RJ, Hodgson L, Condeelis J. Functions of cofilin in cell locomotion and invasion. Nat Rev Mol Cell Biol 2013;14:405–15.
42. Maekawa M, Ishizaki T, Boku S, Watanabe N, Fujita A, Iwamatsu A, et al. Signaling from Rho to the actin cytoskeleton through protein kinases ROCK and LIM-kinase. Science 1999;285:895–8.
43. Arias-Salgado EG, Lizano S, Sarkar S, Brugge JS, Ginsberg MH, Shattil SJ. Src kinase activation by direct interaction with the integrin beta cytoplasmic domain. Proc Natl Acad Sci U S A 2003;100:13298–302.
44. Friedl P, Wolf K. Plasticity of cell migration: a multiscale tuning model. J Cell Biol 2010;188:11–9.
45. Bastea LI, Doppler H, Balogun B, Storz P. Protein kinase D1 maintains the epithelial phenotype by inducing a DNA-bound, inactive SNAI1 transcriptional repressor complex. PLoS One 2012;7:e30459.
46. Eiseler T, Doppler H, Yan IK, Goodison S, Storz P. Protein kinase D1 regulates matrix metalloproteinase expression and inhibits breast cancer cell invasion. Breast Cancer Res 2009;11:R13.
47. Zheng H, Shen M, Zha YL, Li W, Wei Y, Blanco MA, et al. PKD1 phosphorylation-dependent degradation of SNAIL by SCF-FBXO11 regulates epithelial-mesenchymal transition and metastasis. Cancer Cell 2014;26:358–73.
48. Bowden ET, Barth M, Thomas D, Glazer RI, Mueller SC. An invasion-related complex of cortactin, paxillin and PKCmu associates with invadopodia at sites of extracellular matrix degradation. Oncogene 1999;18:4440–9.
49. Karam M, Legay C, Auclair C, Ricort JM. Protein kinase D1 stimulates proliferation and enhances tumorigenesis of MCF-7 human breast cancer cells through a MEK/ERK-dependent signaling pathway. Exp Cell Res 2012;318:558–69.
50. Fu Y, Rubin CS. Protein kinase D: coupling extracellular stimuli to the regulation of cell physiology. EMBO Rep 2011;12:785–96.
51. Spasojevic C, Marangoni E, Vacher S, Assayag F, Meseure D, Chateau-Joubert S, et al. PKD1 is a potential biomarker and therapeutic target in triple-negative breast cancer. Oncotarget 2018;9:23208–19.
52. Karam M, Bieche I, Legay C, Vacher S, Auclair C, Ricort JM. Protein kinase D1 regulates ERalpha-positive breast cancer cell growth response to 17beta-estradiol and contributes to poor prognosis in patients. J Cell Mol Med 2014;18:2536–52.

Published OnlineFirst November 1, 2019; DOI: 10.1158/0008-5472.CAN-18-3241

53. Early Breast Cancer Trialists' Collaborative G, Peto R, Davies C, Godwin J, Gray R, Pan HC, et al. Comparisons between different polychemotherapy regimens for early breast cancer: meta-analyses of long-term outcome among 100,000 women in 123 randomised trials. Lancet 2012;379:432–44.
54. Henderson IC, Berry DA, Demetri GD, Cirrincione CT, Goldstein LJ, Martino S, et al. Improved outcomes from adding sequential paclitaxel but not from escalating doxorubicin dose in an adjuvant chemotherapy regimen for patients with node-positive primary breast cancer. J Clin Oncol 2003;21:976–83.
55. Hayes DF, Thor AD, Dressler LG, Weaver D, Edgerton S, Cowan D, et al. HER2 and response to paclitaxel in node-positive breast cancer. N Engl J Med 2007;357:1496–506.

Published OnlineFirst November 1, 2019; DOI: 10.1158/0008-5472.CAN-18-3241

Cancer Research
The Journal of Cancer Research (1916–1930) | The American Journal of Cancer (1931–1940)

AACR American Association for Cancer Research

Twist1-Induced Epithelial Dissemination Requires Prkd1 Signaling

Dan Georgess, Veena Padmanaban, Orit Katarina Sirka, et al.

Cancer Res 2020;80:204-218. Published OnlineFirst November 1, 2019.